SSRG International Journal of Electrical and Electronics Engineering
ISSN: 2348-8379 / https://doi.org/10.14445/23488379/IJEEE-V11I8P108

Volume 11 Issue 8, 81-90, August 2024

Original Article

Hybrid Deep Learning Segmentation Method on Chest Radiograph Images for Lung Cancer Detection

Raghuram Karla[1], Radhika Yalavarthi[2]

[1,2]*Department of Computer Science and Engineering, Gitam University, Andhra Pradesh, India.*

[1]*Corresponding Author : rkarla@gitam.edu*

Received: 04 June 2024 Revised: 06 July 2024 Accepted: 04 August 2024 Published: 31 August 2024

Abstract *- Chronic pulmonary diseases and lung cancer have become major respiratory concerns in the past decade. Their growing importance emphasizes their impact on public health and the need for better understanding, identification, and control. They increased deaths in India and abroad. High teen and adult smoking rates cause these events. Saving lives requires identifying lung cancer and COPD. Fast and effective diagnosis and treatment of the two disorders. This study employs chest radiographs, neural networks with artificial intelligence, machine learning algorithms, and deep learning techniques to accurately detect the two most lethal thoracic illnesses. Residual neural networks (ResNets) improve picture feature extraction and sickness classification. This approach analyzes chest radiograph imaging scan datasets with anomalies like tiny lobes or larger respiratory system capillaries better than lung imaging. Advanced AI and DL can provide healthcare monitoring systems with accurate insights and results. The dynamic field of oncology uses deep learning techniques. The research focuses on deep learning segmentation models. A model was created to improve chest radiography and lung cancer detection. Investigations using RID data. Model sensitivity and mean false positive are assessed independently. Compared to leading methods, RadiographNet has improved significantly.*

Keywords *- Artificial Intelligence, Arterial infection, Lobes, Pulmonology, Smoking.*

1. Introduction

Presently, there is a worldwide upsurge in the prevalence of cancer, with a notable rise in both the occurrence and death rates of lung cancer [1-3]. Global reports in 2021 indicated a total of 2.37 million individuals diagnosed with lung cancer and 1.76 million fatalities attributed to the disease [4-6]. This concerning pattern emphasizes the crucial requirement for efficient identification and diagnostic techniques to handle better and treat lung cancer.

In the past, the Japan Cancer Research Institute (JCRI) determined that chest radiography and sputum cytology imaging were the most efficient methods for detecting lung cancer [7, 8]. Although these imaging approaches are useful, they present considerable difficulties in achieving precise detection without magnification, resulting in many misdiagnoses. Identifying cancerous cells in these images necessitates a significant level of proficiency and substantial time, which leads to delays and inaccuracies in diagnosis [9].

Although there is ongoing controversy regarding optimal imaging techniques, research indicates that chest CT scans, despite being very affordable, exhibit worse accuracy in comparison to alternative approaches. The main objective of this work is to analyse chest radiograph pictures for early-stage lung cancer detection, as these images are readily accessible and involve lower levels of radiation exposure [10].

CT scans have a significant drawback in the form of a high False Positive Rate (FPR). Low-dose CT scans, as reported by the World Health Organization (WHO), incorrectly label 96% of lesions as false positives. As a result, this results in avoidable subsequent actions and intrusive medical interventions. On the other hand, chest radiography, although less sensitive, has a higher level of specificity compared to chest CT, which makes it a helpful tool for screening lung cancer. Developing a Computer-Aided Diagnosis (CAD) model is crucial for enhancing the precision of cancer identification in chest radiographs. Deep learning models, when applied to chest radiography, have shown enhanced detection results for lung cancer, with sensitivities ranging from 0.51 to 0.84 and mean False Positive Rates (mFPI) between 0.02 and 0.34. Furthermore, these models improve radiologists' capacity to detect nodules, hence decreasing the chances of mistakes.

Radiologists encounter difficulties in differentiating between benign and malignant nodules due to their resemblance to osseous structures. Hence, it is essential to concentrate on the morphological and peripheral

characteristics of nodules. Lesion detection can be influenced by environmental circumstances, which may cause even experienced radiologists to make mistakes. Deep learning approaches, particularly in the areas of detection and segmentation, have a crucial function in the identification of lesions. While detection focuses on classifying pixels, segmentation provides a more detailed categorization at the region level, which improves the performance rate of diagnosis. Although segmentation techniques are feasible to be used in lung cancer detection through chest radiographs, they have not been widely implemented.

The primary goal of this study is to develop and evaluate an advanced deep learning algorithm that uses segmentation techniques to identify lung cancer on chest radiographs accurately. The model prioritizes enhancing sensitivity while minimizing false positives, hence enhancing the early diagnosis and efficacy of treatment.

The primary goals of this study are:

- Creating a sophisticated deep learning system to identify and differentiate lung cancer from chest radiographs precisely.
- The collection's quality is ensured through pixel-level annotation performed by two radiologists, as well as histological investigation to establish the presence of lung cancer nodules and masses.
- Illustrating the enhanced efficacy of segmentation approaches in comparison to classification and detection methods for diagnosing lung cancer and improving treatment outcomes.

2. Literature Study

The utilization of Artificial Intelligence (AI) in the diagnosis, treatment, and management of lung cancer has shown significant promise in recent years. Ladbury et al. [11] examine the progress and practical uses of Artificial Intelligence (AI) in this particular area, emphasizing the capacity of AI to transform the provision of lung cancer treatment. The proposed architecture employs Median and Gaussian filters for preprocessing CT scan images, with the goal of reducing noise and enhancing image quality. The Gaussian noise is distributed discretely throughout the photographs.

The photos that have been treated or polished were segmented using watershed segmentation. During the feature extraction procedure, many characteristics of the cancer nodules that have been discovered, including area, perimeter, eccentricity, centroid, diameter, and pixel mean intensity, have been obtained. The Support Vector Machine (SVM) was utilized to classify the identified nodule as either cancerous or benign. The suggested model has a 92% accuracy in cancer detection and an 86.6% accuracy in cancer classification. Enhancing accuracy can be achieved by implementing appropriate pre-processing methods and eliminating unnecessary objects. The model is inherently complex due to the need for extensive computations to determine the distances between the spots.

El-Brolsy et al. [12] performed a retrospective clinical validation study to assess the efficacy of clinical examination results before and after implementing an artificial intelligence-based Computer-Aided Diagnostic (CAD) system from different vendors. The introduction of the Computer-Aided Design (CAD) system resulted in notable increases in performance metrics. The Computer-Aided Design (CAD) model can detect and emphasize aspects that physicians may have overlooked during their initial evaluation. The Computer-Aided Diagnostic (CAD) system, utilizing artificial intelligence, significantly improved the accuracy of identifying lung cancer nodules on chest radiographs.

Artificial intelligence approaches have shown exceptional effectiveness in assessing cancer images. The researchers examined various classification processes and utilized very efficient segmentation and classification algorithms. The suggested system incorporates an Auto-Encoder system, the OTSU algorithm for segmentation and classification, as well as strong noise filtering approaches like CNN and decision trees. As a result, the system can surpass the limitations that existed in previous detection approaches. The book provides a concise examination of categorization methods, highlighting advancements in LDD technology for the medical industry through the use of the Robust R-CAD system. Additionally, it presents potential ways to address obstacles in future work.

Nanhang et al. and Murugesan et al. [15, 16] investigated various methods for segmenting images, extracting features, and classifying and detecting lung cancer. In the earliest stages, they also compared various strategies. The researchers stated that the CAD system, a continuously evolving technology, assists in the timely identification of cancer by incorporating many inputs from hospitals, including CT scans, X-rays, and MRI scans, together with patients' specific symptoms and biomarkers. Techniques such as Support Vector Machines (SVM), Convolutional Neural Networks (CNN), Artificial Neural Networks (ANN), Watershed Segmentation, and Image Processing are used to improve accuracy and speed up the process.

Alanazi et al., Masud et al., and Amini et al. [17-19] utilized machine learning and image processing methodologies to classify and forecast lung cancer precisely. The first phase entailed gathering photos. Their empirical investigation utilized a dataset including 83 Computed Tomography (CT) scans obtained from a cohort of 70 distinct patients. To enhance the image quality by reducing noise, the geometric mean filter, an image pre-processing technique, was utilized. Subsequently, Linear Discriminant Analysis (LDA)

was utilized. The photos underwent segmentation using the K-means algorithm, which modified both the intensity and texture. Subsequently, categorization tasks were performed using machine learning methods. The Artificial Neural Network (ANN) model was shown to produce the highest accurate predictions for lung cancer. Furthermore, they highlighted the crucial importance of CAD systems in promptly detecting lung cancer.

A deep learning model named LungNet, which integrates Convolutional Neural Networks (CNN) and Recurrent Neural Networks (RNN) to improve the detection and classification of lung cancer nodules was developed. LungNet has demonstrated remarkable precision and durability when compared to traditional methods, making it a very promising tool for the early detection of lung cancer. Moreover, the study emphasized the importance of including geographical and temporal features in order to improve diagnostic outcomes [20].

Furthermore, a multi-task learning framework for the simultaneous detection of lung cancer and COPD from chest X-rays was proposed. The approach employed a Convolutional Neural Network (CNN) backbone that was shared throughout both disorders, along with task-specific layers. This enabled the model to leverage common features for both disorders. The multi-task learning framework showcased the advantages of shared feature learning in medical imaging by attaining enhanced accuracy and efficiency [21].

Agazzi et al., and Ueda et al. have conducted an extensive analysis of the primary methods devised for forecasting lung cancer and identifying nodules through the utilization of CT imaging data. Currently, the most cutting-edge technology available is attained by utilizing Convolutional Neural Networks (CNNs) trained via Deep Learning. With an ample amount of training data, the classification performance is anticipated to reach the low 90s in terms of the Area Under the Curve (AUC) [22, 23].

Chaturvedi et al. are the authors of the mentioned studies. The primary aim of the study was to determine the early stage of lung cancer and evaluate the accuracy of several machine learning techniques [7]. This study employs the TCIA Dataset, Lung Image Database Consortium Image Collection (LIDC-IDRI), and Kaggle data science bowl 2017. The datasets consist of annotated coordinates of nodules for picture segmentation, together with labels indicating their classification as either malignant or non-cancerous.

Deep learning has demonstrated remarkable efficacy in the analysis of medical pictures, accurately recognizing and categorizing lung nodules, extracting distinctive characteristics, and predicting the stage of lung cancer. The first stage of this technology was utilizing image processing techniques to detect and delineate lung areas. The segmentation was performed using the K Means algorithm and the U-Net Convolutional Network. The attributes Diameter, Spiculation, MeanHU, and Eccentricity were derived from the segmented images and can be classified using discretization. The classification was performed using a wide array of machine learning techniques.

Researchers found that classifiers exhibited somewhat better performance than CNN; however, the performance of both systems was comparable. The sensitivity of nodule diagnosis attained by the two-stage neural networks was 65%, which was comparable to the performance demonstrated by radiologists. When comparing neural networks to other systems, it is clear that the rate of false positives is significantly greater, namely at 6.78 per case, by exclusively considering the largest identified nodule for cancer prediction, without taking into account the considerable probability of false positive outcomes. The classifiers have a precision of 41%, which is markedly higher.

3. Materials and Methods

3.1. Dataset

The radiographs are obtained from individuals who have been diagnosed with lung cancer after a pathological examination. A team of expert radiologists interprets the lung cancer lesions observed in the radiograph scan images. The study's findings propose a potential framework for identifying lung cancer using deep learning techniques. The model is trained and validated using radiographs. The model's efficacy was evaluated by using a customized dataset in addition to the original dataset. Two distinct datasets were used during the training phase. Three distinct datasets, namely a train_dataset, a validation_dataset, and a testing_dataset, were generated from the complete dataset [24]. Insertion principles are like (A) a biopsy specimen demonstrating symptomatic, conclusively detected lung cancer; (B) a person aged 40 or above on the pretreatment chest radiograph; and (C) a CT scan of the chest performed within two weeks of the original chest radiograph.

In cases when a patient had multiple chest radiographs that were selected because they satisfied certain criteria, the most recent one was selected. Although the majority of chest radiographs were performed on a regular basis prior to the patient's admission to the hospital, the purpose of these radiographs was not to particularly discover lung cancer. Despite the fact that a CT scan was performed, radiologists did not perform an investigation on chest radiographs that did not reveal the presence of the lesion.

It is generally agreed that the annotations that the radiologists provided are accurate and conclusive. The radiologists employed chest CT images and surgery reports to analyse the features of the lesion. The characteristics encompassed the size, position, and demarcation of the lesion.

If over fifty percent of the edge of the nodule could be followed, it was characterized as having a "traceable edge"; otherwise, it was labeled as having an "untraceable edge".

3.2. Pre-Processing and Augmentation

In order to improve the identification of lung cancer through chest radiographs, it is essential to utilize a sequence of picture preprocessing and augmentation procedures. These strategies enhance image quality and bolster the resilience of deep learning models employed for detection. An image preprocessing technique called Histogram Equalization (HOE) is used. Histogram Equalization is employed to enhance the contrast of chest radiographs by modifying the distribution of intensity in the pictures. Precision is crucial in medical imaging, especially when it comes to distinguishing structures with clarity. The formula for Histogram Equalization (1) can be expressed as follows,

$$I = T * N/P \quad (1)$$

T*N represents the count of pixels at an intensity level ranging from 0 to 255, while P represents the overall count of pixels in the image.

This procedure redistributes the levels of intensity in order to generate a histogram that is homogeneous, therefore improving the contrast of the chest radiographs. The process of equalizing the histogram enhances the visibility of tiny details in lung architecture, making it easier to detect anomalies. Another Pre-processing technique implemented in this work is Adaptive Median Filter (AMF).

The purpose of applying an Adaptive Median Filter to the pictures after histogram equalization is to reduce noise while keeping critical details such as the borders of lung tissues and nodules. The adaptive median filter modifies the size of the neighborhood utilized for filtering in response to the local noise characteristics. This aids in efficiently eliminating noise while preserving the crucial characteristics without causing blurriness. This preprocessing stage leads to clearer and sharper images, which are crucial for precise analysis and identification of lung cancer.

3.2.1. Image Augmentation

Overfitting in Deep Neural Networks is trained on small datasets and is susceptible to overfitting, which occurs when the model learns the irrelevant noise and specific details of the training data instead of extracting broad patterns from it. This can have a detrimental effect on the model's performance when applied to novel, unobserved data. Data augmentation is an effective method for reducing overfitting by artificially enlarging the training dataset using different transformations. Methods for increasing the amount and diversity of data in machine learning tasks. Affine transformations, as described by Pei and Hsiao, are used to create a varied collection of training samples. The transformations encompass rotations, scaling, translations, and shearing, which alter the images while preserving their fundamental characteristics. Offline transformations involve applying techniques such as flipping, rotation, scaling, and cropping to the photos. These modifications contribute to the creation of a diverse dataset, which improves the model's capacity to generalize. The augmented images are compared with the original inputs to confirm that the feature representation remains consistent. This strategy aids in preventing the model from memorizing the enhanced input and facilitates improved generalization.

Technical Specifications

Image Augmentation Pipeline: In the augmentation phase, every chest radiograph goes through many transformations, resulting in a significant number of enhanced samples. One way to achieve this is by using libraries like TensorFlow's ImageDataGenerator or PyTorch's torch-vision transformations, which provide a wide range of capabilities for picture augmentation. To mitigate overfitting, it is crucial to employ a diverse range of augmentation approaches. This encompasses fundamental alterations as well as sophisticated methods such as random wiping, elastic distortions, and color jittering. By combining these strategies, the model is able to acquire resilient features that exhibit strong generalization capabilities when applied to unfamiliar data.

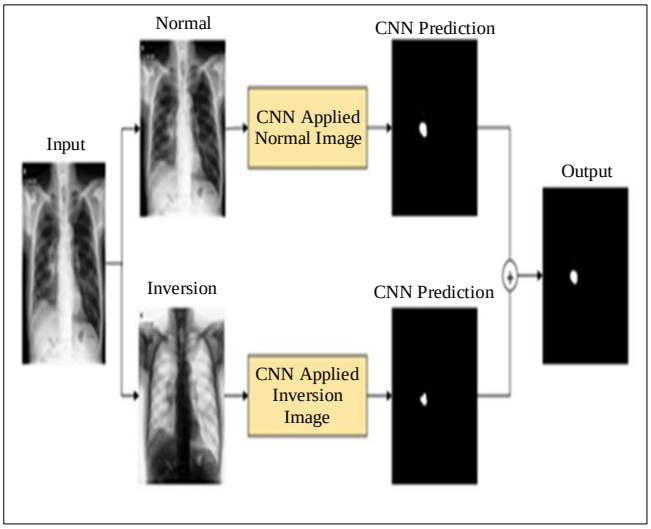

Fig. 1 The outline of the proposed DL-based model

Deep learning algorithms acquire models directly from the given data, making it essential to choose representative image patches for training carefully. Throughout time, numerous methods have been suggested to train deep networks by selecting patches, which include random sampling and tile extraction guided by segmentation. A commonly used procedure involves dividing the target whole slide image into a grid and employing a sliding window technique to extract all the patches for training a Recurrent Neural Network (RNN). A proposed method, the typical architecture shown in Figure 1, involves randomly extracting

a specified number of patches for each class when the image shows an unequal representation of classes. This strategy enables the network to be trained with an equal number of patches for each class, hence avoiding any bias towards a particular class.

3.3. The Proposed Model

This study used a groundbreaking architecture known as a Convolutional Neural Network (CNN) to detect and differentiate abnormal areas in radiograph images accurately. Radiological picture segmentation generates a wide range of characteristics and parameters, in contrast to the detection approach that only identifies the location of the lesion using a bounding box or the categorization strategy that classifies the class based simply on a single image. This is in contrast to the manner of detection. By quantifying the maximum diameter of the lesions, one may accurately determine the stage of the tumors and their growth rate.

This renders it a crucial element in the process of assessing the illness and overseeing the progression of cancer. Moreover, the size of the tumor lesion is often linked to the presence of an oblique orientation, which is defined by departures from both the horizontal and vertical orientations. Relying solely on detection technologies presents significant difficulties in accurately determining the maximal diameter of the lesion.

In order to produce segmented outputs, the CNN architecture is combined with the encoder-decoder architecture, as depicted in Figure 2. The resolution levels of the generated feature maps are reduced as a result of the bottleneck in the encoder-decoder design. Consequently, the model's capacity to handle noise and overfitting is strengthened, resulting in enhanced efficiency.

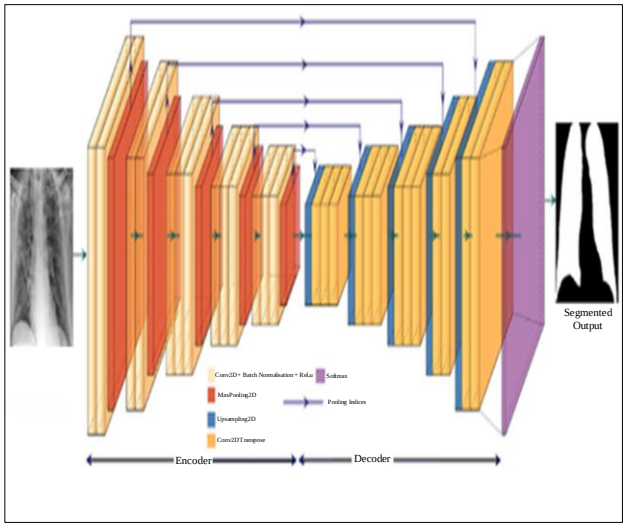

Fig. 2 Encoder-decoder based Convolutional Neural Network (CNN) architecture

The RadiographNet, a deep learning model, can make use of both a traditional chest radiograph and a black and white converted chest radiograph. This attribute is an additional feature of the model. This technique can be seen as a tactic to enhance the model's effectiveness, similar to that of an experienced radiologist. Previous research has demonstrated that in the field of healthcare, reversing the black and white colors in imaging data can help in detecting hidden lesions in visually impaired areas. Based on the study, augmentation is a proven and successful strategy that is implemented in the mode.

The CNN architecture can be applied to both regular radiograph photographs and inverted radiograph pictures. Subsequently, both designs are merged to create the entirety of the model. The loaded image was resized to dimensions of 1536 by 1536. The visual data was enhanced using techniques such as random zooming, shearing, horizontal and vertical shifting, and horizontal flipping. A five-fold cross-validation was performed on chest radiograph pictures that were included in the training dataset in order to evaluate the performance of the proposed model, which was developed from the ground up. In order to achieve the maximum possible degree of performance, the parameters of the suggested model were changed according to the following principles:

rate_of_learning=.0001, Beta_1=.90, Beta_2=.99, Epsilon=0.000001. In addition to that, the model makes use of the Adam optimizer for a period of one hundred epochs. Both Figures 1 and 2 present a schematic representation of the concept that has been suggested. To illustrate the Robin-Marso estimation of the suggested value, Equation (2) is presented.

$$\Sigma_{\{ML\}}^{\{(N)\}} = \Sigma_{\{ML\}}^{\{(N-1)\}} + \frac{1}{N}\left(\left(x_N - \mu_{\{ML\}}^{\{(N)\}}\right)\left(x_N - \mu_{\{ML\}}^{\{(N)\}}\right)^T - \Sigma_{\{ML\}}^{\{(N-1)\}} \right) \quad (2)$$

4. Discussions

This paper introduces a hybrid deep learning method designed to accurately identify lung cancer by analyzing chest radiograph images. Typical architecture is shown in Figure 3. Subsequently, an appraisal of the model's effectiveness is conducted. The model's pixel-level classification technique demonstrates both resilience and efficacy, as it attained a sensitivity of 0.83 and a mean False Positive Index (mFPI) of 0.23 on the test dataset. This illustrates that the model is both efficient and resilient. As far as the author knows, there has been a lack of extensive research undertaken on the segmentation procedure for pathologically diagnosed lung cancer on chest radiographs. This is primarily due to the challenge of discerning the characteristics that are relevant to the inquiry. This study, however, presents a segmentation technique designed to precisely identify lesions in radiological images by utilizing the maximal diameter and oblique orientation.

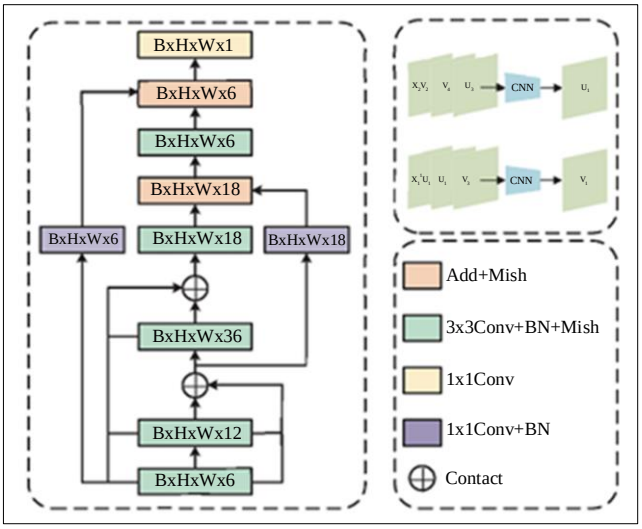

Fig. 3 Illustration of a proposed hybrid method for lung cancer detection

The implementation of classification and detection methodologies in several investigations has successfully led to an accurate diagnosis of lung cancer on chest radiographs. The segmentation strategy not only provides benefits for detection but also offers advantages for measuring the effectiveness of therapy. The segmentation method offers more precise information about the discovered flaws compared to classification or detection methods.

The created approach surpasses previous research in its ability to detect lung cancer, even when using a smaller training sample. This conclusion is significant due to the model's low mFPI. The existing models used in analyzing a training dataset of 5000-18000 radiograph images with nodules or masses yield sensitivity values ranging from 0.51 to 0.84 and mFPI values ranging from 0.02 to 0.34.

Upon retrospectively examining the characteristics of FP deliverables, two notable similarities were identified. Visually, 95% of chest radiograph pictures exhibit nodule or mass-like formations. The model detected a significant number of false positives, which are clusters that resemble nodules and are intertwined with the outlines of ribs and blood vessels. When conducting routine exams, radiologists in clinics often encounter the same issue. Simultaneously, the radiographic photographs exhibit calcified nodules that are superimposed over the normal anatomical structures, leading to an inaccurate diagnosis of the affected structures.

The CT scan not only identified benign calcified lung nodules but also detected five Focal Points (FPs) that were located near the heart, clavicle, or ribs. The presence of these locations was identified following the completion of the CT scan. The model is trained using all of the malignant nodules that have not undergone calcification from the training dataset during the whole training phase.

Subsequently, the calcified nodules are added to the dataset to enhance the reliability of the model. Nevertheless, this was not the prevailing pattern observed in calcified tumors that exhibited similar morphological characteristics. The approach cannot detect the majority of calcified tumors accurately. In other words, the model may incorrectly classify the meningioma as malignant if the calcification features, which are supposed to indicate a non-cancerous growth, are obscured by the typical physical traits of the patient.

An investigation was conducted on the False Negatives (FNs) in the models, revealing that the lesion nodules situated in the blind zones and the metastatic nodules tended to have greater sizes in the model. The proposed model's results indicated a reduction in sensitivity for lesions exhibiting typical morphological traits. This is particularly relevant to regions with restricted visibility.

The system faced challenges in accurately identifying lung cancer images that featured sizable tumors concealed by areas of low visibility. There is a significant correlation between the morphological qualities and the FN photos that show tumors greater than fifty millimeters. Therefore, the model faces challenges in accurately detecting lung cancer, even when it is provided with substantial anatomical features. 33% of the pictures from the FN exhibited the existence of metastatic lesion nodules.

The nodules have a size ranging from 15 to 25 millimeters, with an average of 22 millimeters and a standard deviation of 4.8 millimeters. Conversely, the radiologists originally overlooked most of the tiny nodules that were situated in remote regions. Only once they had acquired a comprehensive comprehension of the precise location and nature of the lung cancer were they able to discern these nodules.

The data used in this methodology was sourced exclusively from a single hospital. It is crucial to examine the potential repercussions that may result from an elevated number of incorrect positive results in a testing group, even while the model has a high ability to detect true positives and a low incidence of incorrectly identifying negatives as positives. To effectively utilize radiographic pictures for therapeutic purposes, the observer must possess a high level of knowledge.

Only lung radiographs showing evidence of malignant tumours or masses were used for this investigation. The research offers several benefits, one of which is the exclusive use of lung tumours that were confirmed to be malignant. Furthermore, the dataset has bitmap annotations generated by two radiologists.

Conversely, it can impede the identification of non-malignant masses and nodules. Regarding the categorization

of non-threatening images, the presented model has few constraints. Generally, this does not pose a problem in terms of practical use. With the exclusion of malignant nodules and masses, it is feasible to instruct all areas as ordinary regions from a technical standpoint.

In order to comprehensively assess the model's performance in real-world clinical settings, it is crucial to incorporate normal images for testing and evaluating the model. The previous sentence indicated that a segmentation-based deep learning algorithm had achieved remarkable accuracy in diagnosing lung cancer on chest radiographs. Chest radiographs offer several advantages over CT scans, such as greater accessibility, lower cost, and reduced radiation exposure for patients.

5. Experiments and Results

The proposed model's performance is assessed on a per-lesion basis to determine the level of malignancy in lung lesions observed in radiography. The model uses a numerical scale ranging from 0 to 255 to determine the likelihood of cancer in a lesion detected in lung nodule images. If the estimated output center of the proposed model falls within the range of the ground truth, it is classified as a True Positive (TP).

A False Positive (FP) occurs when the model generates outcomes that the model did not predict. If the proposed model is capable of calculating two or more True Positives (TPs) even though there is only one ground truth, it is classified as a TP. Whenever the model fails to produce any output for the given image, the False Negative (FN) value is incremented by one. Two radiologists, A.S. and D.U., conducted a retrospective review of the radiograph and CT scan to assess the structures identified by the FP's output.

5.1. Statistical Analysis

An evaluation of the effectiveness of the suggested model is carried out using a lesion-by-lesion approach. We evaluated the accuracy of the model's ability to detect malignant tumours in radiography by analysing the Free-response Receiver-Operating Characteristic (FROC) curve (Figure 4). The FROC curve depicts the sensitivity on the vertical axis and the mFPI on the horizontal axis. To calculate the sensitivity, divide the total amount of actual occurrences by the number of True Positives (TPs) example shown in Figure 5 is reliably identified by the model.

The false positive rate, defined as the ratio of mistakenly recognized positive findings, is calculated by dividing the total number of radiographs in the dataset by the model's false positive rate, the example shown in Figure 7. The statistic is alternatively referred to as the mean false positive rate per image (mFPI) in specific regions. The FROC curve illustrates the positive correlation between variations in sensitivity and the quantity of false positives identified in the image.

5.2. Results Analysis

The suggested model acquired a sensitivity of 0.75 and a mFPI of 0.18 on the test dataset. Figure 4 displays the FROC curve. The mean Intersection Over Union (IOU) of the proposed model is also shown in Figure 6 for various levels of noise. The model attained a maximum sensitivity of 1.00 when applied to tumours with a diameter ranging from 31 to 50 mm.

The model had a sensitivity of 0.85, which ranked as the second-highest among all the tested models for detecting cancers larger than 50 mm in diameter. The sensitivity ratings for lung tumours located in blind locations, such as the pulmonary apices, pulmonary hila, sternum, diaphragm, and subdiaphragmatic region, were found to be 0.51, 0.67, 0.58, 0.51, and 0.60, respectively.

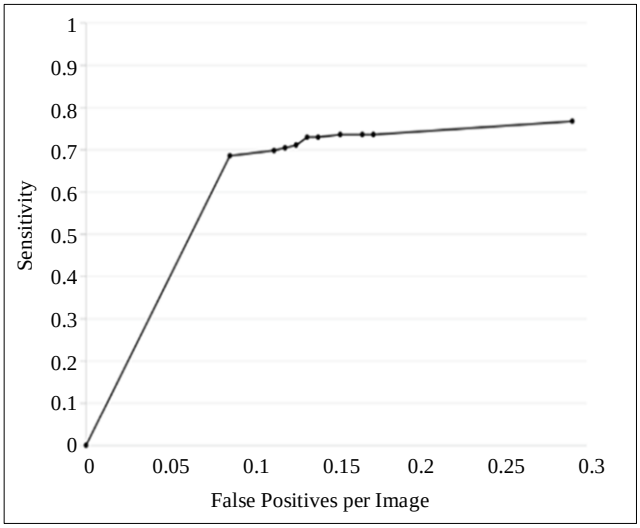

Fig. 4 FROC curve for the test dataset with free-response receiving data

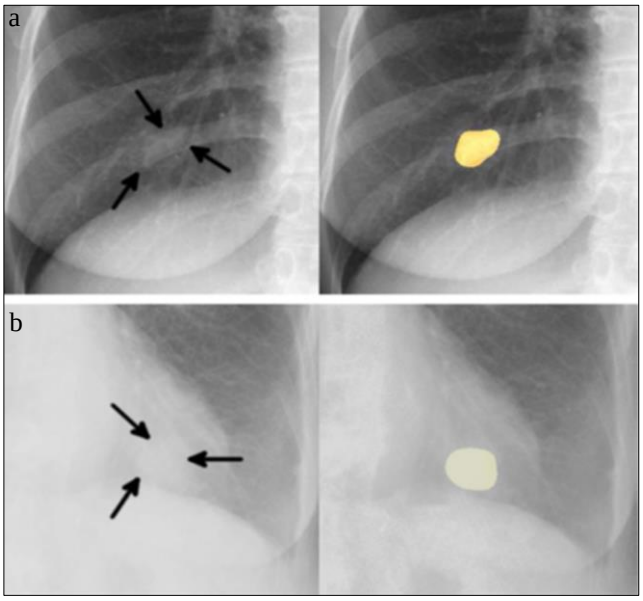

Fig. 5 Two classic examples of true positives

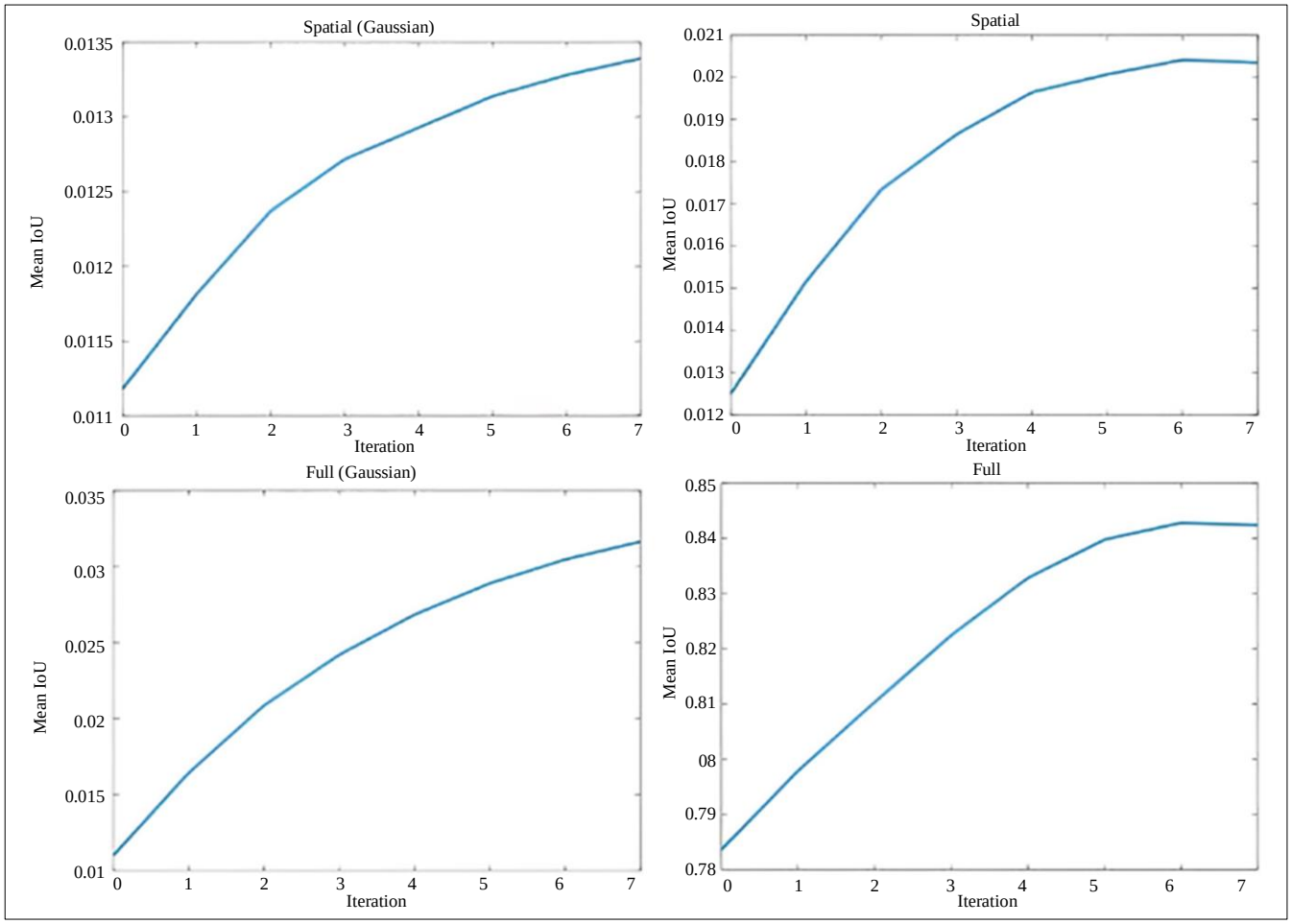

Fig. 6 The mean IOU of the proposed model

The pictures on the left are the originals, while the pictures on the right are the results of the proposed model. The scores were recorded in the order of their respective prevalence. The chest radiographs had a sensitivity of 0.87 for lesions with visible borders, but lesions without borders had a sensitivity of just 0.21. All of the results are displayed in Table 1.

Table 1. Comparative performance of the proposed model with existing models

Classifiers	Accuracy	Error Rate
AlexNet	84.32%	12.30%
VGG16	92.45%	8.70%
GoogleNet	95.32%	5.32%
ResNet	94.89%	2.17%
SVM	95%	3.51%
VGG16	91.45%	9.61%
CheXNet	88%	4%
CNN	89%	15.87%
RadiographNet	96.2%	3.8%

Table 2 shows the effectiveness and defect rates of several classifications employed in the prediction procedure. Even if the majority of classifiers work at a rate of greater than 80%, a growth in error rates decreases their ability to categorize illnesses while also decreasing the effectiveness of the entire system.

Table 2. Specificity and Sensitivity of the existing models

Classifiers	Specificity	Sensitivity
VGG19, SVM	92.41%	93%
Multi Layer perceptron	52.45%	65.41%
CheXNet	NA	82.1%
Artificial Neural Network	89.01%	93.25%
Machine Learning	93.10%	95.61%
Residual Neural Network	92.07%	92.71%
Support Vector Machine	91.15%	92%
Progressive Dense V- N/w	83.10%	NA
VGG16	94.00%	NA
MobileNet	84%	81.2%
RadiographNet (Proposed model)	96.02%	96.5%

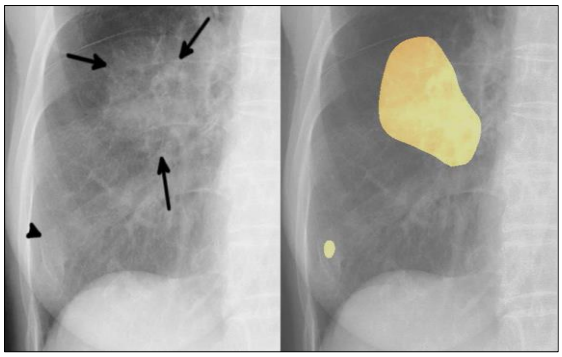

Fig. 7 Solitary instance of an FP

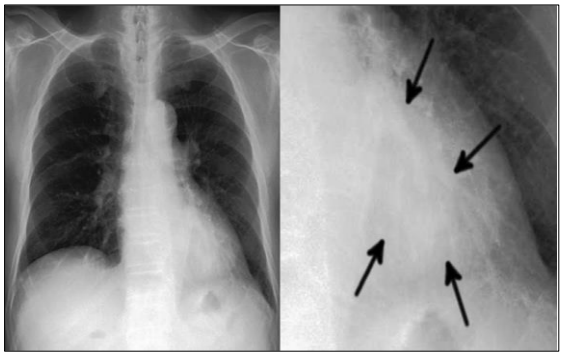

Fig. 8 FN case example

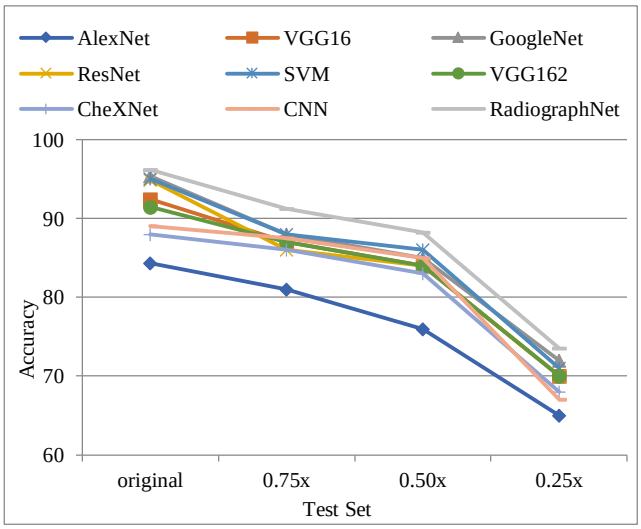

Fig. 9 HOG graph of the proposed under different constraints

The average dice coefficient for a total of 152 lesions was 0.52, with a standard deviation of 0.37. Out of the 112 detected lesions, the model found that the average dice coefficient was 0.76, with a standard deviation of 0.24. The dataset includes the remaining seventy-one lesions that intersect with the blind areas and have an average dice coefficient ranging from 0.36 to 0.44. Out of the entire collection of lesions in the dataset, 39 of them are situated in areas that were not part of the training set. The average coefficient of the dice is approximately 0.74, with a potential margin of error of 0.16. By analyzing the chest radiograph, highly experienced radiologists successfully detected 19 out of the 20 False Positives (FPs). Thirteen of the twenty false positives are linked to locations that are not perceptible to the unaided eye. In total, there were 43 false negatives, with 32 of them occurring alongside blind zones. Additionally, there were 34 spots with no visibility. The average size of the FNs was 31.75 millimeters, with dimensions ranging from 8 to 70 millimeters. Four FNs, each measuring over fifty millimeters, were reported to be located between blind zones. In Figure 8, there was a case of lung cancer that was not detected (false negative) at the same time as a visual blind spot. In Figure 8, there was a result that incorrectly indicated the presence of cancer (false positive) and was placed on top of normal anatomical components. Both of these outcomes are displayed here. Figure 9 displays the HOG graph.

6. Conclusion

Overall, this study introduces a hybrid deep learning model that utilizes a fundamental Convolutional Neural Network (CNN) to analyze the greatest diameter dimension for precise diagnosis of lung cancer in pre-diagnosed cases. Through the utilization of a segmentation strategy, the model improves the resilience of categorization and effectively captures all pertinent information. The hybrid CNN model exhibited improved performance compared to other approaches, as indicated by its greater accuracy, specificity, sensitivity, F1-score, and Area Under the Curve (AUC). These technological developments empower medical professionals to diagnose lung cancer accurately. Subsequent investigations could examine the utilization of deep learning methodologies to ascertain the extent of lung cancer severity and expedite prompt diagnosis. Nevertheless, the suggested model also exhibits a degree of intricacy, which may create difficulties during its execution.

References

[1] Yong Han et al., "Histologic Subtype Classification of Non-Small Cell Lung Cancer Using PET/CT Images," *European Journal of Nuclear Medicine and Molecular Imaging*, vol. 48, pp. 350-360, 2021. [CrossRef] [Google Scholar] [Publisher Link]

[2] Isaac Shiri et al., Impact of Feature Harmonization on Radio Genomics Analysis: Prediction of EGFR and KRAS Mutations from Non-Small Cell Lung Cancer PET/CT Images," *Computers in Biology and Medicine*, vol. 142, pp. 1-12, 2022. [CrossRef] [Google Scholar] [Publisher Link]

[3] Tiening Zhang et al., "Simultaneous Identification of EGFR, KRAS, ERBB2, and TP53 Mutations in Patients with Non-Small Cell Lung Cancer by Machine Learning-Derived Three-Dimensional Radionics," *Cancers*, vol. 13, no. 8, pp. 1-14, 2021. [CrossRef] [Google Scholar] [Publisher Link]

[4] Marjolein A. Heuvelmans et al., "Lung Cancer Prediction by Deep Learning to Identify Benign Lung Nodules," *Lung Cancer*, vol. 154, pp. 1-4, 2021. [CrossRef] [Google Scholar] [Publisher Link]

[5] Beung-Chul Ahn et al., Clinical Decision Support Algorithm Based on Machine Learning to Assess the Clinical Response to Anti-Programmed Death-1 Therapy in Patients with Non–Small-Cell Lung Cancer," *European Journal of Cancer*, vol. 153, pp. 179-189, 2021. [CrossRef] [Google Scholar] [Publisher Link]

[6] Margarita Kirienko et al., "Radiomics and Gene Expression Profiles to Characterise the Disease and Predict Outcomes in Patients with Lung Cancer," *European Journal of Nuclear Medicine and Molecular Imaging*, vol. 48, pp. 3643-3655, 2021. [CrossRef] [Google Scholar] [Publisher Link]

[7] Pragya Chaturvedi et al., "Prediction and Classification of Lung Cancer Using Machine Learning Techniques," *IOP Conference Series: Materials Science and Engineering*, vol. 1099, 2021. [CrossRef] [Google Scholar] [Publisher Link]

[8] Apurva Singh, Rhea Chitalia, and Despina Kontos, "Radiogenomics in Brain, Breast, and Lung Cancer: Opportunities and Challenges," *Journal of Medical Imaging*, vol. 8, no. 3, 2021. [CrossRef] [Google Scholar] [Publisher Link]

[9] Ichidai Tanaka, Taiki Furukawa, and Masahiro Morise, "The Current Issues and Future Perspective of Artificial Intelligence for Developing New Treatment Strategy in Non-Small Cell Lung Cancer: Harmonization of Molecular Cancer Biology and Artificial Intelligence," *Cancer Cell International*, vol. 21, no. 1, pp. 1-14, 2021. [CrossRef] [Google Scholar] [Publisher Link]

[10] Panagiotis Marentakis et al., "Lung Cancer Histology Classification from CT Images Based on Radiomics and Deep Learning Models," *Medical & Biological Engineering & Computing*, vol. 59, pp. 215-226, 2021. [CrossRef] [Google Scholar] [Publisher Link]

[11] Colton Ladbury et al., "Integration of Artificial Intelligence in Lung Cancer: Rise of the Machine," *Cell Reports Medicine*, pp. 1-11, 2023. [CrossRef] [Google Scholar] [Publisher Link]

[12] Hanaa Mohammed Elsayed Mohammed El-Brolsy et al., "Fighting Non-Small Lung Cancer Cells Using Optimal Functionalization of Targeted Carbon Quantum Dots Derived from Natural Sources Might Provide Potential Therapeutic and Cancer Bio-Image Strategies," *International Journal of Molecular Sciences*, vol. 23, no. 21, pp. 1-23, 2022. [CrossRef] [Google Scholar] [Publisher Link]

[13] Ilke Tunali, Robert J. Gillies, and Matthew B. Schabath, "Application of Radiomics and Artificial Intelligence for Lung Cancer Precision Medicine," *Cold Spring Harbor Perspectives in Medicine*, vol. 14, no. 8, pp. 1-25, 2021. [CrossRef] [Google Scholar] [Publisher Link]

[14] Chintakayala Tejaswini et al., "CNN Architecture for Lung Cancer Detection," *2022 IEEE 11th International Conference on Communication Systems and Network Technologies (CSNT)*, Indore, India, pp. 346-350, 2022. [CrossRef] [Google Scholar] [Publisher Link]

[15] Nanhang Zhu et al., "A Light-Up Fluorescence Resonance Energy Transfer Magnetic Aptamer Sensor for Ultra-Sensitive Lung Cancer Exosome Detection," *Journal of Materials Chemistry B*, vol. 9, pp. 2483-2493, 2021. [CrossRef] [Google Scholar] [Publisher Link]

[16] Malathi Murugesan et al., "A Hybrid Deep Learning Model for Effective Segmentation and Classification of Lung Nodules from CT Images," *Journal of Intelligent & Fuzzy Systems*, vol. 42, no. 3, pp. 2667-2679, 2022. [CrossRef] [Google Scholar] [Publisher Link]

[17] Saad Awadh Alanazi et al., "Boosting Breast Cancer Detection Using Convolutional Neural Network," *Journal of Healthcare Engineering*, vol. 2021, pp. 1-11, 2021. [CrossRef] [Publisher Link]

[18] Mehedi Masud et al., "A Machine Learning Approach to Diagnosing Lung and Colon Cancer Using A Deep Learning-Based Classification Framework," *Sensors*, vol. 21, no. 3, pp. 1-20, 2021. [CrossRef] [Google Scholar] [Publisher Link]

[19] Mehdi Amini et al., "Overall Survival Prognostic Modelling of Non-Small Cell Lung Cancer Patients Using Positron Emission Tomography/Computed Tomography Harmonised Radionics Features: the Quest for the Optimal Machine Learning Algorithm," *Clinical Oncology*, vol. 34, no. 2, pp. 114-127, 2022. [CrossRef] [Google Scholar] [Publisher Link]

[20] Shalini Wankhade, and S. Vigneshwari, "A Novel Hybrid Deep Learning Method for Early Detection of Lung Cancer Using Neural Networks," *Healthcare Analytics*, vol. 3, pp. 1-13, 2023. [CrossRef] [Google Scholar] [Publisher Link]

[21] G.M.F. Wallace et al., "Chest X-Rays in COPD Screening: Are they Worthwhile?," *Respiratory Medicine*, vol. 103, no. 12, pp. 1862-1865, 2009. [CrossRef] [Google Scholar] [Publisher Link]

[22] Giorgio Maria Agazzi et al., "CT Texture Analysis for Prediction of EGFR Mutational Status and ALK Rearrangement in Patients with Non-Small Cell Lung Cancer," *La Radiologia Medica*, vol. 126, pp. 786-794, 2021. [CrossRef] [Google Scholar] [Publisher Link]

[23] Daiju Ueda et al., "Artificial Intelligence-Supported Lung Cancer Detection by Multi-Institutional Readers with Multi-Vendor Chest Radiographs: A Retrospective Clinical Validation Study," *BMC Cancer*, vol. 21, pp. 1-8, 2021. [CrossRef] [Google Scholar] [Publisher Link]

[24] Samuel G. Armato III et al., "The Lung Image Database Consortium (LIDC) and Image Database Resource Initiative (IDRI): A Completed Reference Database of Lung Nodules on CT Scans," *The International Journal of Medical Physics Research and Practice*, vol. 38, no. 2, pp. 915-931, 2011. [CrossRef] [Google Scholar] [Publisher Link]

[25] Tafadzwa L. Chaunzwa et al., "Deep Learning Classification of Lung Cancer Histology Using CT Images," *Scientific Reports*, vol. 11, pp. 1-12, 2021. [CrossRef] [Google Scholar] [Publisher Link]